

## Quadruple band MIMO dielectric resonator antenna for 5G SUB-6 GHz applications

Nur Atika Bazadry<sup>1</sup>, Hasliza A Rahim<sup>2,3</sup>, Mohd Najib Mohd Yasin<sup>2,3</sup>, Mohamedfareq Abdulmalek<sup>4</sup>

<sup>1</sup>TM ELIT Department, GITN Putrajaya Campus Network (PCN), Putrajaya, Malaysia

<sup>2</sup>Advanced Communication Engineering, Centre of Excellence (ACE), Universiti Malaysia Perlis (UniMAP), Kangar, Malaysia

<sup>3</sup>Department of Electronic, Faculty of Electronic Engineering and Technology, Universiti Malaysia Perlis (UniMAP), Arau, Malaysia

<sup>4</sup>Faculty of Engineering and Information Sciences, University of Wollongong in Dubai, Dubai, United Arab Emirates

### Article Info

#### Article history:

Received Sep 10, 2021

Revised Aug 30, 2022

Accepted Sep 12, 2022

#### Keywords:

5G bands

Antenna and propagation

Bioelectromagnetics

Dielectric resonator antenna

Multiple-input-multiple-output

Wearable antenna

### ABSTRACT

A quadruple band with L-slotted multiple-input-multiple-output (MIMO) square dielectric resonator antenna (SDRA) for fifth generation (5G) applications at the sub-6 GHz band is presented, which can cover 5G new radio band N77 (3.3–4.2) GHz and N79 (4.4–5) GHz. The proposed structure consists of a single SDRA mounted on a substrate excited by an aperture slot underneath dielectric resonators (DR)s. The performance of SDRA is improved by introducing L-shaped slot on the central part of DRA. Results show that the MIMO SDRA antenna achieves  $S_{11} < -10$  dB and  $S_{21} < -15$  dB for all resonant frequencies at 3.5 GHz, 4 GHz, 4.6 GHz, and 5 GHz, indicating good performance of the antenna at the desired frequencies. The maximum realized gain is 5.61 dB and 5.01 dB at port 1, 4 GHz and port 2, 4.6 GHz, respectively. The radiation efficiencies are acceptable for all resonant frequencies. Moreover, the proposed antenna design achieved good envelop correlation coefficient (ECC) and diversity gain (DG) at the desired frequencies. Thus, the antenna can be used for 5G sub-6 GHz applications.

This is an open access article under the [CC BY-SA](https://creativecommons.org/licenses/by-sa/4.0/) license.



### Corresponding Author:

Hasliza A Rahim

Department of Electronic, Faculty of Electronic Engineering and Technology

Universiti Malaysia Perlis (UniMAP)

Kampus Alam Unimap, Arau 02600, Perlis, Malaysia

Email: haslizarahim@unimap.edu.my

## 1. INTRODUCTION

Wireless communication has taken an enormous improvement and development to acquire data and share information in the life of humankind. Due to the tremendous increase in demand by the users and also to suit the current trends, a significant development needs to be implemented to fulfill the Fifth Generation (5G) wireless communication requirement. However, the requirement of 5G wireless communication technologies poses many challenges for antennas [1]-[9] regarding particular antennas' configuration, fabrication, and integration criteria. 5G will expand wireless broadband services through the high-speed optical fiber communication as the backbone, surpassing mobile internet access towards the internet of things (IoT) and device-to-device communications [10], [11] for many applications such as global positioning system (GPS) [12], radiofrequency (RF) energy harvesting [13] and embedded system [14]. Dielectric resonator antenna (DRA) [15]-[25] has gained extensive attention due to its attractive characteristics and has become the preferred choice for a good radiator since it offers a high radiation efficiency and wider bandwidth. As wireless communication technology evolves, the need to implement the multi-band operation antenna for MIMO applications has increased where many research studies are based on the DRA-MIMO

where many techniques were introduced to obtain the multi-band operation in MIMO [19]-[24]. Most of the research studies present the use of more than one element of DRA to form a MIMO antenna which will cause the antenna size to be large [25]. Since the spacing between the elements needs to be considered to obtain good isolation, using fewer elements is needed. To our best knowledge, this is the first quadruple band, L-slotted using the DR material. The antenna can provide quadruple band coverage for 5G new radio band N77 (3.3-4.2) GHz and N79 (4.4-5) GHz.

**2. METHOD**

A simple geometric structure of a single element MIMO SDRA in Figure 1 is illustrated in Figure 1(a). Meanwhile, Figure 1(b) shows the perspective view of SDRA and Figure 1(c) shows the top and rear views of SDRA. The antenna topology is made up of Alumina ( $\epsilon_{r,Alumina}=10, \tan\delta=0.002$ ) in a square with a thickness,  $H_{dra}=17$  mm. The DRA is placed on top of the substrate composed of FR4 ( $\epsilon_{r,FR4}=4.7, \tan\delta=0.02$ ) with a thickness,  $t=1.6$  mm. The dimension of the MIMO SDRA is  $44 \times 44$  mm<sup>2</sup>. The important parameters of the proposed antenna dimensions are tabulated in Table 1. A slot is notched on the ground, and at the bottom of the FR4 substrate, an L-shaped monopole microstrip feeding is etched.

Table 1. Parameters and dimensions of the proposed MIMO SDRA

Parameter	Value (mm)	Parameter	Value (mm)
Wg	100	Hdra	17
Lg	100	gt	0.035
Wsub	100	h	1.6
Lsub	100	Wfeed	3
Wdra	44	Lfeed	46
Ldra	44	Hslot	30
Wslot	2.44	b	24
Lslot	22	c	6

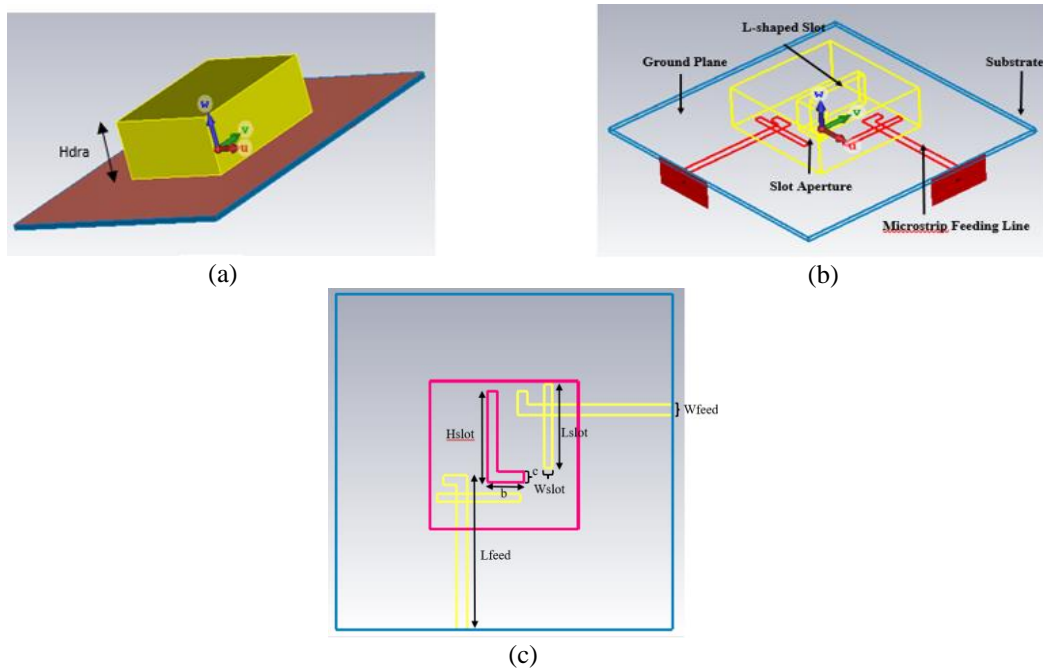


Figure 1. Topology of MIMO SDRA in different views (a) perspective view without L-slot, (b) perspective view with L-slot, and (c) top view (left) and rear view (right)

**3. RESULTS AND DISCUSSION**

This section presents the results of the proposed MIMO SDRA in terms of critical parameter assessments and the optimized results of crucial parameters. Such investigations were performed for three selected parameters. The discussion of the obtained results is included in this section.

### 3.1. Critical parameters assessments

In this section, three critical parameters of the proposed SDRA, such as the size of the substrate, L-shaped slotted dimensions (height and length), and length of the aperture slot, are studied and investigated. Other parameters are kept constant at a time. This analysis is done to observe the changes in  $S_{11}$  and  $S_{21}$  parameters. The first investigation is conducted on the effect of the dimensions of the substrate on the result of reflection coefficient ( $S_{11}$ ). As for transmission coefficient ( $S_{21}$ ), the reference will be at -15 dB. Figure 2 shows the results of  $S_{11}$  and  $S_{21}$  for substrate of difference dimensions; which the first design, the substrate is  $200 \times 200 \text{ mm}^2$  and the other design is  $100 \times 100 \text{ mm}^2$ . As the substrate size increases, the frequency shifts towards higher frequencies, as shown in Figure 2(a). In contrast, the frequency shifts down towards the lower frequencies when the substrate size reduces. At 3.5 GHz,  $S_{11}$  value for substrate size at  $100 \times 100 \text{ mm}^2$  is -10.10 dB. However, when the size of the substrate is made larger at  $200 \times 200 \text{ mm}^2$ , the  $S_{11}$  is improved,  $S_{11} = -15.35 \text{ dB}$ . This variation demonstrates that substrate size critically affects the return loss value for lower band frequency, 3.5 GHz. However, return loss is affected severely by the increased substrate size for the upper band 4.6 GHz. At this resonant frequency, the  $S_{11}$  value for  $200 \times 200 \text{ mm}^2$  is -9.80 dB in which it does not surpass the reference level ( $S_{11} < -10 \text{ dB}$ ). The value of  $S_{11}$  for substrate size of  $100 \times 100 \text{ mm}^2$  improves to -22.89 dB by up to 2.3 times compared to substrate size of  $200 \times 200 \text{ mm}^2$ . The acceptable  $S_{11}$  and  $S_{21}$  values are achieved when the substrate size is  $100 \times 100 \text{ mm}^2$ , as shown in Figure 2(a) and Figure 2(b), respectively.

Second, several variations have been made to the L-shaped slotted in order to get acceptable results for all key parameters, as illustrated in Figure 3 and Figure 4. In this critical parameter assessment, the position of the slotted is fixed. The varied values of height are  $H_{\text{slot}} = \{26.5, 27.7, 28.9, 30\} \text{ mm}$ . Figure 4 shows the results of  $S_{11}$  and  $S_{21}$  when varying the L-shaped slotted length,  $b = \{18, 20, 22, 24\} \text{ mm}$ .

Figure 3(a) shows that  $H_{\text{slot}}$  gives significant effect on the upper band, 5 GHz, when the  $H_{\text{slot}}$  decreases in terms of  $S_{11}$ . The lower bands are not affected by the variation of  $H_{\text{slot}}$ . On the contrary, when  $H_{\text{slot}}$  decreases,  $S_{21}$  values reduce slightly for two upper bands, 4.6 GHz and 5 GHz, as shown in Figure 3(b). Thus, it is shown that the upper bands can be controlled by tuning the dimensions of  $H_{\text{slot}}$  without affecting the lower bands.

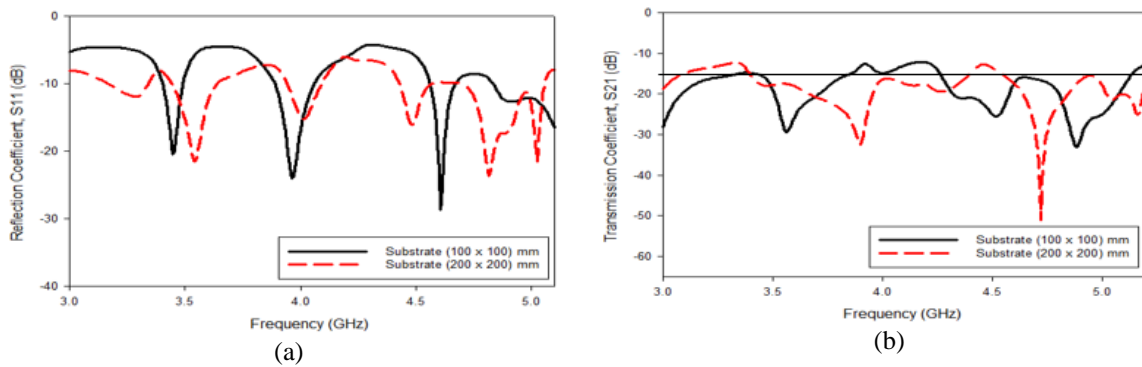


Figure 2. Performance of MIMO SDRA by varying substrate size (a)  $S_{11}$  and (b)  $S_{21}$

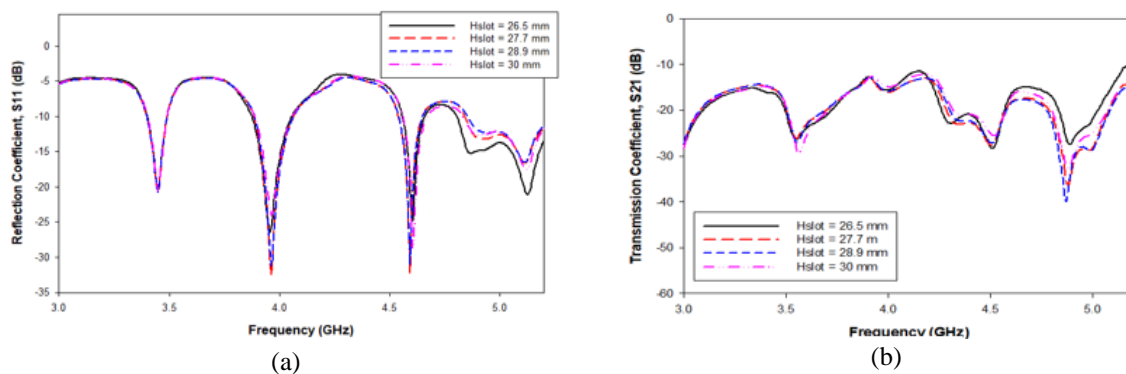


Figure 3. Performance of MIMO SDRA by varying height of L-shaped slotted,  $H_{\text{slot}}$  (a)  $S_{11}$  and (b)  $S_{21}$

Figure 4(a) shows that when the  $b$  increases,  $S_{11}$  is almost unchanged. However, shifts downwards with increasing  $b$  for the upper bands, 4.6 GHz and 5 GHz. The  $S_{21}$  also remain consistent with a slight decrease when the length of  $b$  is extended, as illustrated in Figure 4(b). This indicates that the upper band can be fine-tuned by varying the values of  $b$  without changing the performance of the lower band. Thus,  $b = 24$  mm is chosen.

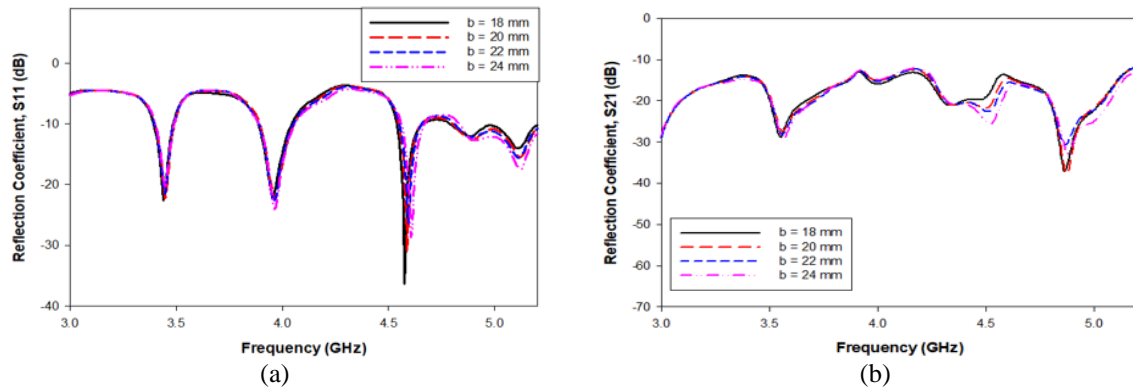


Figure 4. Performance of MIMO SDRA by varying values of L-shaped slotted length (a)  $S_{11}$  and (b)  $S_{21}$

### 3.2. Free space simulation

The results demonstrate that the  $S_{11}$  values for all operating frequency bands are well below -10 dB. The results of both  $S_{11}$  and  $S_{21}$  for the optimized design of the proposed MIMO SDRA are shown in Table 2. Table 3 presents the simulated results for realized gain and radiation efficiency. The peak gain obtained at port 1 is 5.61 dB at 4 GHz, while at port 2, the peak gain achieved is 5.01 dB at 4.6 GHz. The overall value of gains across the desired frequency bands are obtained higher than 4 dB, indicating the good performance of the proposed MIMO SDRA. Good radiation efficiencies are achieved at port 1 across the resonant frequencies as the radiation efficiencies are more than 60%. Similarly, in port 2, the radiation efficiencies are more than 40%. However, the radiation efficiency deteriorates slightly for the resonant frequency at 5 GHz, given by 33.28%. The radiation pattern for the proposed MIMO SDRA is plotted in both E-plane and H-plane for both ports. The results show that all the proposed MIMO SDRA's directions transmit or receive the radiofrequency (RF) signals in the outwards direction, both for ports 1 and 2, as shown in Table 4. The direction of the antenna beam is slightly tilted to  $30^\circ$  for port 1 and port 2 at 4.6 GHz and 5 GHz, respectively. However, the beam of MIMO SDRA is also tilted  $60^\circ$  to the right at 5 GHz, port 1.

Table 2. Results of S-parameters for optimized MIMO SDRA

Antenna parameters	Frequency (GHz)			
	3.5	4	4.6	5
$S_{11}$ (dB)	-10.10	-16.92	-22.85	-12.15
$S_{21}$ (dB)	-19.18	-15.00	-17.30	-24.96

Table 3. Gain and radiation efficiency of the proposed MIMO SDRA

Antenna Parameters		Frequency (GHz)			
		3.5	4	4.6	5
Gain (dB)	Port 1	4.25	5.61	3.43	4.32
	Port 2	4.31	4.56	5.01	3.11
Radiation efficiency (%)	Port 1	71.73	76.24	74.31	64.04
	Port 2	61.26	65.11	63.80	33.28

The analysis of diversity performance parameters is also presented to investigate the performance of MIMO characteristics for SDRA. Figure 5 shows the graph of simulated ECC and DG. The ECC and DG are two significant parameters to take into account while assessing the diversity characteristics of MIMO performances. ECC (optimally  $< 0.5$ ) is normally used to determine the degree of similarity and correlation between the two identities. The ECC can be calculated by S-parameters, expressed as (1).

$$ECC(\rho_e) = \frac{|S_{11}^* S_{12} + S_{11} S_{22}^*|}{(1 - |S_{11}|^2 + |S_{21}|^2)(1 - |S_{22}|^2 + |S_{12}|^2)} \tag{1}$$

The value of DG can be calculated as (2).

$$DG = 10\sqrt{1 - |0.99\rho_e|} \tag{2}$$

Ideally, the value of DG obtained should be closer to 10 dB. ECCs at all resonant frequencies are below 0.05 and satisfy the minimum diversity criteria (< 0.5), as shown in Figure 5(a). A low ECC contributes to high DG, as shown in Figure 5(b). The obtained DG is almost 10 dB.

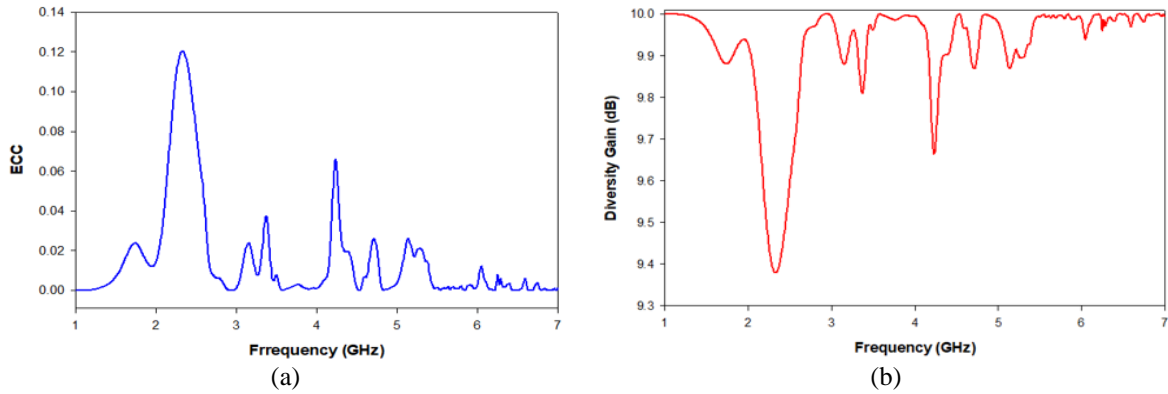


Figure 5. MIMO diversity of the MIMO SDRA (a) ECC and (b) DG

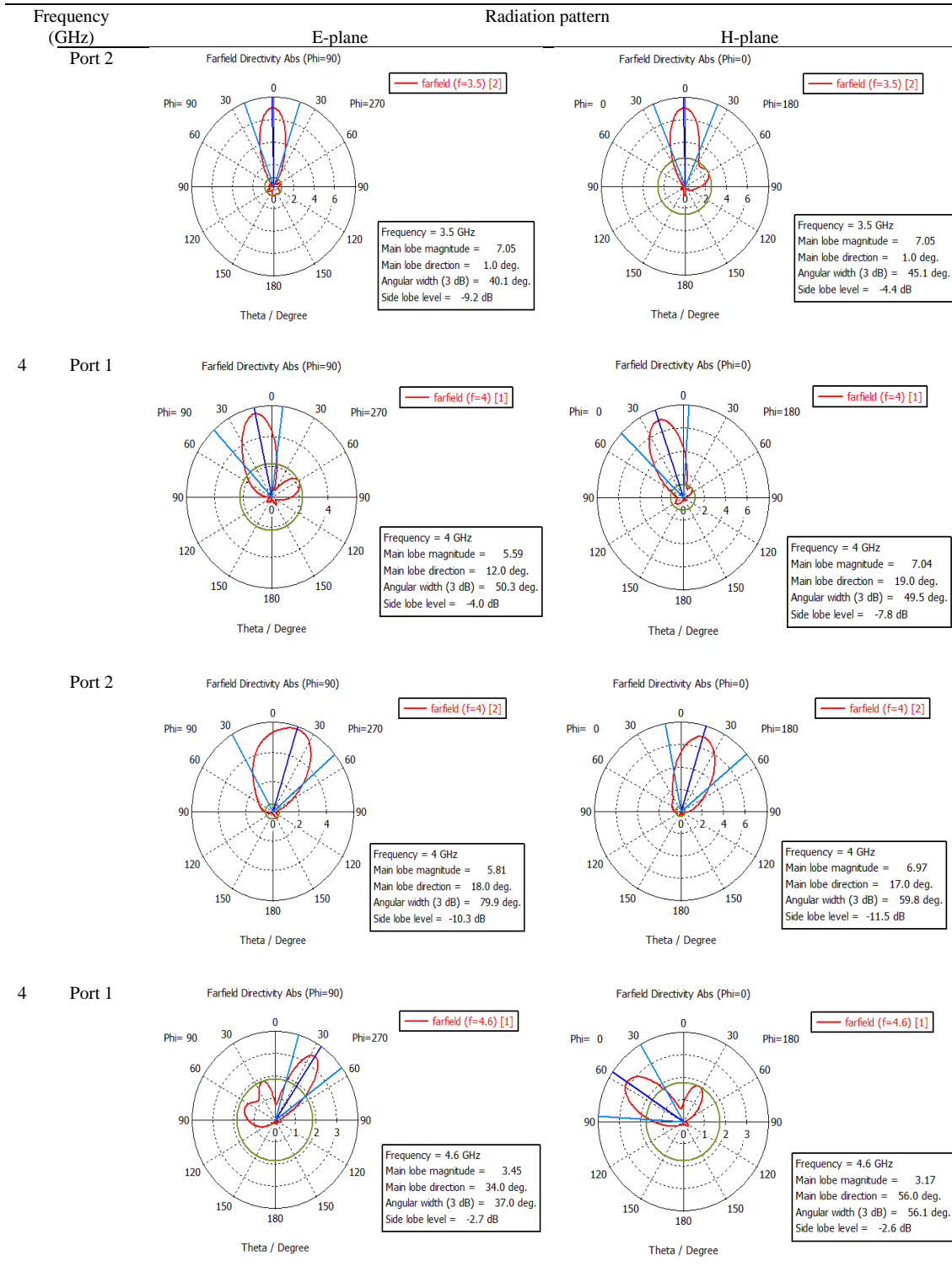
#### 4. CONCLUSION

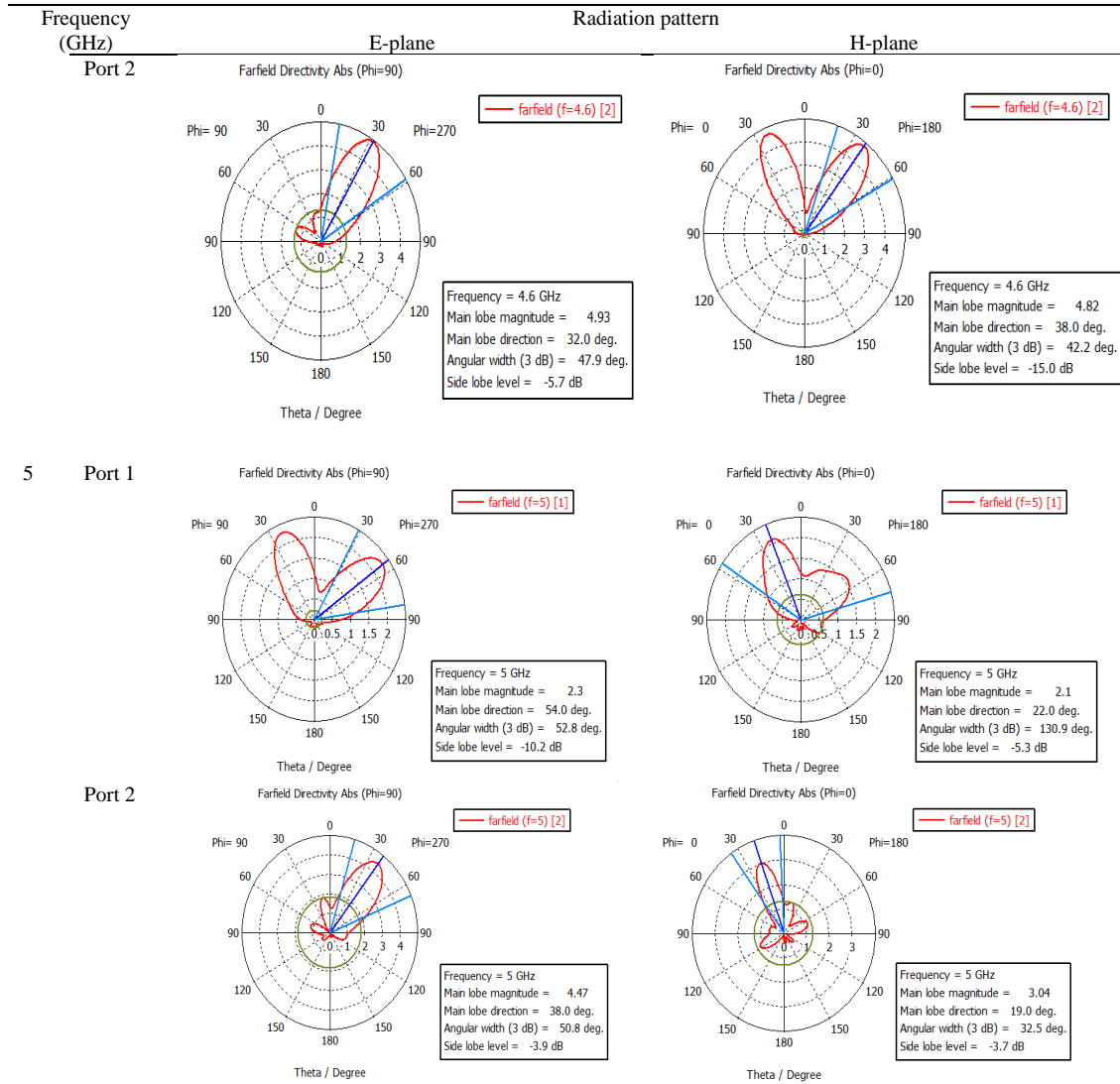
This paper presents a quadruple band L-slotted MIMO SDRA that operates at four distinct resonant frequencies, which are 3.5 GHz, 4 GHz, 4.6 GHz, and 5 GHz for 5G sub-6 GHz applications. The findings show that the proposed MIMO SDRA exhibits good performance in terms of  $S_{11}$ ,  $S_{21}$ , realized gain, radiation efficiency, ECC, and DG.

#### APPENDIX

Table 4. Radiation patterns in E-Plane and H-Plane of the proposed MIMO SDRA

Frequency (GHz)	Radiation pattern	
	E-plane	H-plane
3.5 Port 1	<p>Farfield Directivity Abs (Phi=90)</p> <p>— farfield (f=3.5) [1]</p> <p>Frequency = 3.5 GHz Main lobe magnitude = 5.88 Main lobe direction = 48.0 deg. Angular width (3 dB) = 68.5 deg. Side lobe level = -7.7 dB</p>	<p>Farfield Directivity Abs (Phi=0)</p> <p>— farfield (f=3.5) [1]</p> <p>Frequency = 3.5 GHz Main lobe magnitude = 2.3 Main lobe direction = 0.0 deg. Angular width (3 dB) = 33.9 deg. Side lobe level = -1.1 dB</p>





## ACKNOWLEDGEMENTS

The authors of this paper wish to acknowledge the support from ACE and Department of Electronic, Faculty of Electronic Engineering & Technology, Universiti Malaysia Perlis (UniMAP).

## REFERENCES

- [1] A. Ramos, T. Varum, and J. N. Matos, "Compact multilayer yagi-uda based antenna for IoT/5G sensors," *Sensors*, vol. 18, Article no. 2914, 2018, doi: 10.3390/s18092914.
- [2] E. L. Bengtsson, F. Rusek, S. Malkowsky, F. Tufvesson, P. C. Karlsson, and O. Edfors, "A simulation framework for multiple-antenna terminals in 5G massive MIMO systems," *IEEE Access* vol. 5, pp. 26819–26831, 2017, doi: 10.1109/ACCESS.2017.2775210.
- [3] M. M. Rahman, M. S. Islam, H. Y. Wong, T. Alam, and M. T. Islam, "Performance analysis of a defected ground-structured antenna loaded with stub-slot for 5G communication," *Sensors*, vol. 19, Article no. 2634, 2019, doi: 10.3390/s19112634
- [4] S. Fakhte, H. Oraizi, and L. Matekovits, "Gain improvement of rectangular dielectric resonator antenna by engraving grooves on its side walls," *IEEE Antennas and Wireless Propagation Letters*, vol. 16, pp. 2167–2170, 2017, doi: 10.1109/LAWP.2017.2702584.
- [5] C.-H. Li and T.-Y. Chiu, "340-GHz low-cost and high-gain on-chip higher order mode dielectric resonator antenna for THz applications," *IEEE Transactions on Terahertz Science and Technology*, vol. 7, pp. 284–294, 2017, doi: 10.1109/TTHZ.2017.2670234.
- [6] H. A. Rahim *et al.*, "Effect of different substrate materials on a wearable textile monopole antenna," *2012 IEEE Symposium on Wireless Technology and Applications (ISWTA)*, 2012, pp. 245–247, doi: 10.1109/ISWTA.2012.6373853.
- [7] D. Hou *et al.*, "D-band on-chip higher-order-mode dielectric-resonator antennas fed by half-mode cavity in CMOS technology," *IEEE Antennas and Propagation Magazine*, vol. 56, no. 3, pp.80–89, 2014, doi: 10.1109/MAP.2014.6867684.

- [8] T. Dabas, D. Gangwar, B. K. Kanaujia, and A. K. Gautam, "Mutual coupling reduction between elements of UWB MIMO antenna using small size uniplanar EBG exhibiting multiple stop bands," *AEU - International Journal of Electronics and Communications*, vol. 93, pp. 32–38, 2018, doi: 10.1016/j.aeue.2018.05.033.
- [9] H. A. Rahim, M. Abdulmalek, P. J. Soh, and G. A. E. Vandenbosch, "Evaluation of a broadband textile monopole antenna performance for subject specific on-body applications," *Applied Physics A*, vol. 123, Article no. 97, 2017, doi: 10.1007/s00339-016-0680-9.
- [10] N. H. Shahadan *et al.*, "Steerable higher order mode dielectric resonator antenna with parasitic elements for 5G applications," *IEEE Access*, vol. 5, pp. 22234–22243, 2017, doi: 10.1109/ACCESS.2017.2760924.
- [11] M. Farahani, M. Akbari, M. Nedil, and T. A. Denidni, "Mutual coupling reduction in dielectric resonator MIMO antenna arrays using metasurface orthogonalize wall," *2017 11th European Conference on Antennas and Propagation (EUCAP)*, pp. 985–987, 2017, doi: 10.1109/ACCESS.2017.2760924.
- [12] M. I. Jais *et al.*, "1.575 GHz dual-polarization textile antenna (DPTA) for GPS application," *2013 IEEE Symposium on Wireless Technology & Applications (ISWTA)*, 2013, pp. 376–379, doi: 10.1109/ISWTA.2013.6688808.
- [13] I. Adam, M. F. A. Malek, M. N. M. Yasin, and H. A. Rahim, "Double band microwave rectifier for energy harvesting," *Microwave and Optical Technology Letters*, vol. 58, no. 4, pp. 922–927, 2016, doi: 10.1002/mop.29709.
- [14] M. I. Ahmad, Z. Husin, R. B. Ahmad, H. A. Rahim, M. S. A. Hassan and M. N. Md Isa, "FPGA based control IC for multilevel inverter," in *2008 International Conference on Computer and Communication Engineering*, 2008, pp. 319–322, doi: 10.1109/ICCCE.2008.4580620.
- [15] N. Al Shalaby and S. El-Sherbiny, "Mutual coupling reduction of DRA for MIMO applications," *Advanced Electromagnetics*, vol. 8, no. 1, pp. 75–81, 2019, doi: 10.7716/aem.v8i1.730.
- [16] Y. Zhang, J.-Y. Deng, M.-J. Li, D. Sun, and L.-X. Guo, "A MIMO dielectric resonator antenna with improved isolation for 5G mm-Wave applications," *IEEE Antennas and Wireless Propagation Letters*, vol. 18, no. 4, pp. 747–751, 2019, doi: 10.1109/LAWP.2019.2901961.
- [17] N. K. Mishra, J. Acharjee, V. Sharma, C. Tamrakar, and L. Dewangan, "Mutual coupling reduction between the cylindrical dielectric resonator antenna using split ring resonator based structure," *AEU - International Journal of Electronics and Communications*, vol. 154, 2022, doi: 10.1016/j.aeue.2022.154305.
- [18] G. Das, A. Sharma, and R. K. Gangwar, "Dielectric resonator-based two-element MIMO antenna system with dual band characteristics," *IET Microwaves, Antennas & Propagation*, vol. 12, no. 5, pp. 734–741, 2018, doi: 10.1049/iet-map.2017.0744.
- [19] A. Abdalrazik, A. S. A. El-Hameed, and A. B. Abdel-Rahman, "A three-port MIMO dielectric resonator antenna using decoupled modes," *IEEE Antennas and Wireless Propagation Letters*, vol. 16, pp. 3104–3107, 2017, doi: 10.1109/LAWP.2017.2763426.
- [20] Q. Guo and J. Zhang, "A dual-band rectangular dielectric resonator antenna array for 5G applications," *2019 IEEE MTT-S International Wireless Symposium (IWS)*, 2019, pp. 1–3, doi: 10.1109/IEEE-IWS.2019.8804084.
- [21] M. D. Alanazi and S. K. Khamas, "A compact dual band MIMO dielectric resonator antenna with improved performance for mm-Wave applications," *Sensors*, vol. 22, no. 13, 2022, doi: 10.3390/s22135056.
- [22] A. Sharma, G. Das, and R. K. Gangwar, "Design and analysis of tri-band dual-port dielectric resonator based hybrid antenna for WLAN/WiMAX applications," *IET Microwaves, Antennas & Propagation*, vol. 12, no. 6, pp. 986–992, 2018, doi: 10.1049/iet-map.2017.0822.
- [23] S. U. Anuar, M. H. Jamaluddin, J. Din, K. Kamardin, M. H. Dahri, and I. H. Idris, "Triple band MIMO dielectric resonator antenna for LTE applications," *AEU - International Journal of Electronics and Communications*, vol. 118, p. 153172, 2020, doi: 10.1016/j.aeue.2020.153172.
- [24] A. A. Khan, M. H. Jamaluddin, S. Aqeel, J. Nasir, J. U. R. Kazim, and O. Owais, "Dual-band MIMO dielectric resonator antenna for WiMAX/WLAN applications," *IET Microwaves, Antennas & Propagation*, vol. 11, no. 1, pp. 113–120, 2017, doi: 10.1049/iet-map.2015.0745.
- [25] J. Nasir, M. H. Jamaluddin, M. Khalily, M. R. Kamarudin, and I. Ullah, "Design of an MIMO dielectric resonator antenna for 4G applications," *Wireless Personal Communications*, vol. 88, no. 3, pp. 525–536, 2016, doi: 10.1007/s11277-016-3174-3.

## BIOGRAPHIES OF AUTHORS



**Nur Atika Bazadry**    received bachelor's degree (Communication Engineering) from Universiti Malaysia Perlis (UniMAP), Perlis, Malaysia, in 2021. She is currently working with TM ELIT Department, GITN Putrajaya Campus Network (PCN). Her research interests include dielectric resonator antenna and wearable antenna. She can be contacted at email: nuratika.bazadry@gmail.com.



**Hasliza A Rahim**    received the bachelor's degree in electrical engineering from the University of Southern California, Los Angeles, CA, USA, in 2003, the master's degree in electronics design system from Universiti Sains Malaysia, Pulau Pinang, Malaysia, in 2006, and the Ph.D. degree in communication engineering from Universiti Malaysia Perlis, Perlis, Malaysia, in 2015. In 2006, she joined School of Computer and Communication Engineering (SCCE), Universiti Malaysia Perlis (UniMAP), as a Lecturer, where she is currently an Associate Professor with Faculty of Electronic Engineering & Technology. Her research interests include wearable and conformal antennas, metamaterials, antenna, and propagation, and bioelectromagnetics. She can be contacted at email: haslizarahim@unimap.edu.my.



**Mohd Najib Mohd Yasin**    received the M.Eng. degree in electronic engineering from the University of Sheffield, United Kingdom, and the Ph.D. degree from the University of Sheffield, Sheffield, U.K., in 2007 and 2013, respectively. Since 2013, he has been a Lecturer in the School of Microelectronics, Universiti Malaysia Perlis, Malaysia. His research interests include computational electromagnetics, conformal antennas, mutual coupling, wireless power transfer, array design, and dielectric resonator antennas. He can be contacted at email: najibyasini@unimap.edu.my.



**Mohamedfareq Abdulmalek**    is an Associate Professor in the Faculty of Engineering and Information Sciences at University of Wollongong in Dubai (UOWD), Dubai, UAE. Before he joined UOWD, Dr Mohd Fareq worked for Universiti Malaysia Perlis (Dean, School of Electrical Systems Engineering). To date, he has published 381 peer-reviewed scientific publications. His work has been cited more than 4165 times and with an h-index of 30. He can be contacted at email: mohamedfareqmalek@uowdubai.ac.ae.